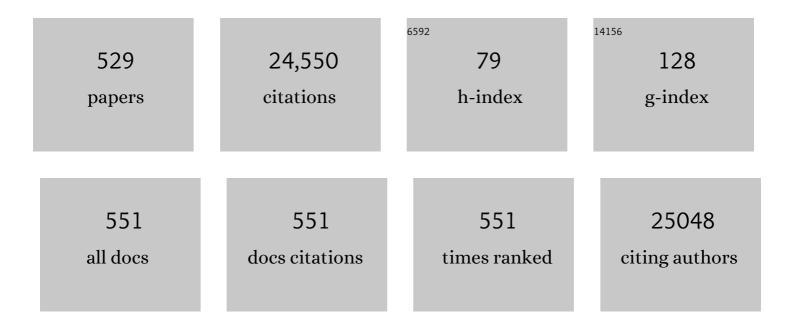
## Zdenek Sofer

List of Publications by Year in descending order

Source: https://exaly.com/author-pdf/3061601/publications.pdf Version: 2024-02-01



#	Article	IF	CITATIONS
1	Highly exfoliated NiPS3 nanosheets as efficient electrocatalyst for high yield ammonia production. Chemical Engineering Journal, 2022, 430, 132649.	6.6	17
2	Enhanced voltammetric performance of sensors based on oxidized 2D layered black phosphorus. Talanta, 2022, 238, 123036.	2.9	3
3	Synthesis and Applications of Graphene Oxide. Materials, 2022, 15, 920.	1.3	121
4	Simultaneous microwave-assisted reduction and B/N co-doping of graphene oxide for selective recognition of VOCs. Journal of Materials Chemistry C, 2022, 10, 3307-3317.	2.7	5
5	Prospective advances in MXene inks: screen printable sediments for flexible micro-supercapacitor applications. Journal of Materials Chemistry A, 2022, 10, 4533-4557.	5.2	38
6	Dealloying layered PdBi <sub>2</sub> nanoflakes to palladium hydride leads to enhanced electrocatalytic N <sub>2</sub> reduction. Journal of Materials Chemistry A, 2022, 10, 11904-11916.	5.2	6
7	Exfoliated Fe3GeTe2 and Ni3GeTe2 materials as water splitting electrocatalysts. FlatChem, 2022, 32, 100334.	2.8	11
8	Allâ€Solutionâ€Processed Van der Waals Heterostructures for Waferâ€Scale Electronics. Advanced Materials, 2022, 34, e2106110.	11.1	43
9	Energetic Au ion beam implantation of ZnO nanopillars for optical response modulation. Journal Physics D: Applied Physics, 2022, 55, 215101.	1.3	2
10	Biohybrid Micro- and Nanorobots for Intelligent Drug Delivery. Cyborg and Bionic Systems, 2022, 2022,	3.7	28
11	Fine-tuning the functionality of reduced graphene oxide via bipolar electrochemistry in freestanding 2D reaction layers. Carbon, 2022, 191, 439-447.	5.4	8
12	InSe:Ge-doped InSe van der Waals heterostructure to enhance photogenerated carrier separation for self-powered photoelectrochemical-type photodetectors. Nanoscale, 2022, 14, 5412-5424.	2.8	9
13	Microstructural modifications induced in Si <sup>+</sup> -implanted yttria-stabilised zirconia: a combined RBS-C, XRD and Raman investigation. Physical Chemistry Chemical Physics, 2022, 24, 6290-6301.	1.3	0
14	Sulfonated NbS <sub>2</sub> -based proton-exchange membranes for vanadium redox flow batteries. Nanoscale, 2022, 14, 6152-6161.	2.8	8
15	High-Entropy NASICON Phosphates (Na <sub>3</sub> M <sub>2</sub> (PO <sub>4</sub> ) <sub>3</sub> and) Tj I Inorganic Chemistry, 2022, 61, 4092-4101.	ETQq1 1 ( 1.9	0.784314 rg 23
16	Simple Bottom-Up Synthesis of Bismuthene Nanostructures with a Suitable Morphology for Competitive Performance in the Electrocatalytic Nitrogen Reduction Reaction. Inorganic Chemistry, 2022, 61, 5524-5538.	1.9	9
17	2D Heterostructures for Highly Efficient Photodetectors: From Advanced Synthesis to Characterizations, Mechanisms, and Device Applications. Advanced Photonics Research, 2022, 3, .	1.7	13
18	Synthesis of Magnesium Phosphorous Trichalcogenides and Applications in Photoelectrochemical Water Splitting. Small, 2022, 18, e2200355.	5.2	8

#	Article	IF	CITATIONS
19	Transition metal dichalcogenides as catalysts for the hydrogen evolution reaction: The emblematic case of "inert―ZrSe <sub>2</sub> as catalyst for electrolyzers. Nano Select, 2022, 3, 1069-1081.	1.9	6
20	Photomodification of benzyl germanane with group 6 metal carbonyls. FlatChem, 2022, 33, 100354.	2.8	2
21	Flexible, ultralight, and high-energy density electrochemical capacitors using sustainable materials. Electrochimica Acta, 2022, 415, 140239.	2.6	12
22	Topochemical Transformation of Two-Dimensional VSe <sub>2</sub> into Metallic Nonlayered VO <sub>2</sub> for Water Splitting Reactions in Acidic and Alkaline Media. ACS Nano, 2022, 16, 351-367.	7.3	23
23	PtSe <sub>2</sub> on a reduced graphene oxide foil for the alkaline hydrogen evolution reaction. Materials Advances, 2022, 3, 4348-4358.	2.6	6
24	The multi-energetic Au ion implantation of graphene oxide and polymers. EPJ Web of Conferences, 2022, 261, 02006.	0.1	2
25	Electroactive nanocarbon materials as signaling tags for electrochemical PCR. Talanta, 2022, 245, 123479.	2.9	2
26	Synthesis, characterisation, and feasibility studies on the use of vanadium tellurate( <scp>vi</scp> ) as a cathode material for aqueous rechargeable Zn-ion batteries. RSC Advances, 2022, 12, 12211-12218.	1.7	2
27	Layered selenophosphate HgPSe <sub>3</sub> single crystals: a new candidate for X-ray to visible light photodetectors. Journal of Materials Chemistry C, 2022, 10, 8834-8844.	2.7	2
28	Electromagnetic Interference Shielding by Reduced Graphene Oxide Foils. ACS Applied Nano Materials, 2022, 5, 6792-6800.	2.4	13
29	Stimuli-responsive of magnetic metal-organic frameworks (MMOF): Synthesis, dispersion control, and its tunability into polymer matrix under the augmented-magnetic field for H2 separation and CO2 capturing applications. International Journal of Hydrogen Energy, 2022, 47, 20166-20175.	3.8	4
30	Coâ€doping Graphene with B and N Heteroatoms for Application in Energy Conversion and Storage Devices. ChemNanoMat, 2022, 8, .	1.5	8
31	Layer-Dependent Interlayer Antiferromagnetic Spin Reorientation in Air-Stable Semiconductor CrSBr. ACS Nano, 2022, 16, 11876-11883.	7.3	22
32	Oleic acid/oleylamine ligand pair: a versatile combination in the synthesis of colloidal nanoparticles. Nanoscale Horizons, 2022, 7, 941-1015.	4.1	61
33	Liquid-Phase Exfoliation of Magnetically and Optoelectronically Active Ruthenium Trichloride Nanosheets. ACS Nano, 2022, 16, 11315-11324.	7.3	10
34	Improving C–N–FeO <sub><i>x</i></sub> Oxygen Evolution Electrocatalysts through Hydroxyl-Modulated Local Coordination Environment. ACS Catalysis, 2022, 12, 7443-7452.	5.5	12
35	Antimony nanomaterials modified screen-printed electrodes for the voltammetric determination of metal ions. Electrochimica Acta, 2022, 425, 140690.	2.6	9
36	Arsenene and Antimonene. , 2022, , 149-172.		0

#	Article	IF	CITATIONS
37	Chiral molecular intercalation superlattices. Nature, 2022, 606, 902-908.	13.7	67
38	Electrochemical Behavior of Rechargeable Al–Ni Battery Systems in Concentrated [EMIm]Cl-AlCl <sub>3</sub> Electrolyte. ACS Applied Energy Materials, 2022, 5, 6797-6804.	2.5	0
39	Vanadium Dopants: A Boon or a Bane for Molybdenum Dichalcogenidesâ€Based Electrocatalysis Applications. Advanced Functional Materials, 2021, 31, 2009083.	7.8	14
40	Modification of structure and surface morphology in various ZnO facets via low fluence gold swift heavy ion irradiation. Surface and Interface Analysis, 2021, 53, 230-243.	0.8	1
41	Surface Engineering Strategy Using Urea To Improve the Rate Performance of Na <sub>2</sub> Ti <sub>3</sub> O <sub>7</sub> in Naâ€lon Batteries. Chemistry - A European Journal, 2021, 27, 3875-3886.	1.7	14
42	Nanoconfined deep eutectic solvent in laminated MXene for efficient CO2 separation. Chemical Engineering Journal, 2021, 405, 126961.	6.6	56
43	Intrinsic carrier multiplication in layered Bi2O2Se avalanche photodiodes with gain bandwidth product exceeding 1 GHz. Nano Research, 2021, 14, 1961-1966.	5.8	17
44	Self-reconstruction mediates isolated Pt tailored nanoframes for highly efficient catalysis. Journal of Materials Chemistry A, 2021, 9, 22501-22508.	5.2	5
45	Lithium-Assisted Exfoliation of Palladium Thiophosphate Nanosheets for Photoelectrocatalytic Water Splitting. ACS Applied Nano Materials, 2021, 4, 441-448.	2.4	8
46	MoS <sub>2</sub> stacking matters: 3R polytype significantly outperforms 2H MoS <sub>2</sub> for the hydrogen evolution reaction. Nanoscale, 2021, 13, 19391-19398.	2.8	16
47	Functionalized metallic transition metal dichalcogenide (TaS <sub>2</sub> ) for nanocomposite membranes in direct methanol fuel cells. Journal of Materials Chemistry A, 2021, 9, 6368-6381.	5.2	22
48	Electrochemical Exfoliation of Janus-like BiTel Nanosheets for Electrocatalytic Nitrogen Reduction. ACS Applied Nano Materials, 2021, 4, 590-599.	2.4	12
49	Effect of surface chemistry on bio-conjugation and bio-recognition abilities of 2D germanene materials. Nanoscale, 2021, 13, 1893-1903.	2.8	13
50	Rhenium Doping of Layered Transition-Metal Diselenides Triggers Enhancement of Photoelectrochemical Activity. ACS Nano, 2021, 15, 2374-2385.	7.3	19
51	Liquid Metalsâ€Assisted Synthesis of Scalable 2D Nanomaterials: Prospective Sediment Inks for Screenâ€Printed Energy Storage Applications. Advanced Functional Materials, 2021, 31, 2010320.	7.8	26
52	6FDA-DAM:DABA Co-Polyimide Mixed Matrix Membranes with GO and ZIF-8 Mixtures for Effective CO2/CH4 Separation. Nanomaterials, 2021, 11, 668.	1.9	24
53	Molybdenum Oxide Supported on Ti <sub>3</sub> AlC <sub>2</sub> is an Active Reverse Water–Gas Shift Catalyst. ACS Sustainable Chemistry and Engineering, 2021, 9, 4957-4966.	3.2	15
54	Atomically Thin Nanosheets Confined in 2D Heterostructures: Metalâ€ion Batteries Prospective. Advanced Energy Materials, 2021, 11, 2100451.	10.2	35

#	Article	IF	CITATIONS
55	Prediction Clue on the Fading Capacity of Multi-Walled Carbon Nanotube-Decorated Li <sub>2</sub> (Fe <sub>1–<i>x</i></sub> Ti <sub><i>x</i></sub> )SiO <sub>4</sub> /C High-Performance Cathode Materials. Energy & Fuels, 2021, 35, 8321-8333.	2.5	13
56	Picric Acid Violet Light Assisted Photodegradation Mediated by Germanene-Based Materials. Bulletin of the Chemical Society of Japan, 2021, 94, 1695-1701.	2.0	5
57	Photoelectrochemical Activity of Layered Metal Phosphorous Trichalcogenides for Water Oxidation. Advanced Materials Interfaces, 2021, 8, 2100294.	1.9	8
58	Functionalized Germanene-Based Nanomaterials for the Detection of Single Nucleotide Polymorphism. ACS Applied Nano Materials, 2021, 4, 5164-5175.	2.4	17
59	Two-Dimensional Gallium Sulfide Nanoflakes for UV-Selective Photoelectrochemical-type Photodetectors. Journal of Physical Chemistry C, 2021, 125, 11857-11866.	1.5	41
60	Cobalt Phosphorous Trisulfide as a High-Performance Electrocatalyst for the Oxygen Evolution Reaction. ACS Applied Materials & amp; Interfaces, 2021, 13, 23638-23646.	4.0	31
61	Carbonaceous Oxygen Evolution Reaction Catalysts: From Defect and Dopingâ€Induced Activity over Hybrid Compounds to Ordered Framework Structures. Small, 2021, 17, e2007484.	5.2	25
62	Interfacial Covalent Bonds Regulated Electronâ€Deficient 2D Black Phosphorus for Electrocatalytic Oxygen Reactions. Advanced Materials, 2021, 33, e2008752.	11.1	56
63	Phosphorene and other layered pnictogens as a new source of 2D materials for electrochemical sensors. TrAC - Trends in Analytical Chemistry, 2021, 139, 116249.	5.8	25
64	Ambient-Stable Two-Dimensional Crl <sub>3</sub> <i>via</i> Organic-Inorganic Encapsulation. ACS Nano, 2021, 15, 10659-10667.	7.3	20
65	Self-Powered Broadband Photodetector and Sensor Based on Novel Few-Layered Pd <sub>3</sub> (PS <sub>4</sub> ) <sub>2</sub> Nanosheets. ACS Applied Materials & Interfaces, 2021, 13, 30806-30817.	4.0	13
66	Ruthenium on Alkaliâ€Exfoliated Ti <sub>3</sub> (Al <sub>0.8</sub> Sn <sub>0.2</sub> )C <sub>2</sub> MAX Phase Catalyses Reduction of 4â€Nitroaniline with Ammonia Borane. ChemCatChem, 2021, 13, 3470-3478.	1.8	6
67	Photocatalytic activity of twist-angle stacked 2D TaS2. Npj 2D Materials and Applications, 2021, 5, .	3.9	12
68	High-yield exfoliation of 2D semiconductor monolayers and reassembly of organic/inorganic artificial superlattices. CheM, 2021, 7, 1887-1902.	5.8	36
69	Chiral Phonons and Giant Magnetoâ€Optical Effect in CrBr <sub>3</sub> 2D Magnet. Advanced Materials, 2021, 33, e2101618.	11.1	31
70	Direct Observation of Magnon-Phonon Strong Coupling in Two-Dimensional Antiferromagnet at High Magnetic Fields. Physical Review Letters, 2021, 127, 097401.	2.9	54
71	Layered ZnIn <sub>2</sub> S <sub>4</sub> Single Crystals for Ultrasensitive and Wearable Photodetectors. Advanced Optical Materials, 2021, 9, 2100845.	3.6	17
72	CeO2-Blended Cellulose Triacetate Mixed-Matrix Membranes for Selective CO2 Separation. Membranes, 2021, 11, 632.	1.4	11

#	Article	IF	CITATIONS
73	Overcoming the Challenges of Freestanding Tin Oxideâ€Based Composite Anodes to Achieve High Capacity and Increased Cycling Stability. Advanced Functional Materials, 2021, 31, 2106373.	7.8	9
74	The Role of Alkali Cation Intercalates on the Electrochemical Characteristics of Nb <sub>2</sub> CT <sub><i>X</i></sub> MXene for Energy Storage. Chemistry - A European Journal, 2021, 27, 13235-13241.	1.7	9
75	A short investigation on LiMn2O4 wrapped with MWCNT as composite cathode for lithium-ion batteries. Bulletin of Materials Science, 2021, 44, 1.	0.8	1
76	Integration of BiOI nanosheets into bubble-propelled micromotors for efficient water purification. FlatChem, 2021, 30, 100294.	2.8	9
77	Nitrogen-doped graphene based triboelectric nanogenerators. Nano Energy, 2021, 87, 106173.	8.2	30
78	Edge-Hydrogenated Germanene by Electrochemical Decalcification-Exfoliation of CaGe <sub>2</sub> : Germanene-Enabled Vapor Sensor. ACS Nano, 2021, 15, 16709-16718.	7.3	15
79	Comparison between layered Pt3Te4 and PtTe2 for electrocatalytic reduction reactions. FlatChem, 2021, 29, 100280.	2.8	22
80	Modified Single-Walled Carbon Nanotube Membranes for the Elimination of Antibiotics from Water. Membranes, 2021, 11, 720.	1.4	9
81	Understanding electrochemical capacitors with in-situ techniques. Renewable and Sustainable Energy Reviews, 2021, 149, 111418.	8.2	32
82	Molecular-level fabrication of highly selective composite ZIF-8-CNT-PDMS membranes for effective CO2/N2, CO2/H2 and olefin/paraffin separations. Separation and Purification Technology, 2021, 274, 119003.	3.9	27
83	Sub-millimetre scale Van der Waals single-crystal MoTe2 for potassium storage: Electrochemical properties, and its failure and structure evolution mechanisms. Energy Storage Materials, 2021, 43, 284-292.	9.5	17
84	Inverted perovskite solar cells with enhanced lifetime and thermal stability enabled by a metallic tantalum disulfide buffer layer. Nanoscale Advances, 2021, 3, 3124-3135.	2.2	23
85	Liquidâ€Phase Exfoliated Gallium Selenide for Lightâ€Driven Thinâ€Film Transistors. Advanced Electronic Materials, 2021, 7, 2001080.	2.6	18
86	Functionalized germanane/SWCNT hybrid films as flexible anodes for lithium-ion batteries. Nanoscale Advances, 2021, 3, 4440-4446.	2.2	13
87	Surface Modification by High-Energy Heavy-Ion Irradiation in Various Crystalline ZnO Facets. Physical Chemistry Chemical Physics, 2021, 23, 22673-22684.	1.3	5
88	Colloidal chemical bottom-up synthesis routes of pnictogen (As, Sb, Bi) nanostructures with tailored properties and applications: a summary of the state of the art and main insights. CrystEngComm, 2021, 23, 7876-7898.	1.3	11
89	The effectiveness of Soxhlet extraction as a simple method for GO rinsing as a precursor of high-quality graphene. Nanoscale Advances, 2021, 3, 5292-5300.	2.2	4
90	Surface oxidation of Ti <sub>3</sub> C <sub>2</sub> T <sub>x</sub> enhances the catalytic activity of supported platinum nanoparticles in ammonia borane hydrolysis. 2D Materials, 2021, 8, 015001.	2.0	17

#	Article	IF	CITATIONS
91	Improved CO2/CH4 Separation Properties of Cellulose Triacetate Mixed–Matrix Membranes with CeO2@GO Hybrid Fillers. Membranes, 2021, 11, 777.	1.4	10
92	Mineralizer-free synthesis of orthorhombic arsenic-phosphorus alloys. FlatChem, 2021, 30, 100297.	2.8	4
93	Heat-Up Colloidal Synthesis of Shape-Controlled Cu-Se-S Nanostructures—Role of Precursor and Surfactant Reactivity and Performance in N2 Electroreduction. Nanomaterials, 2021, 11, 3369.	1.9	6
94	Lightâ€Driven ZnO Brushâ€Shaped Selfâ€Propelled Micromachines for Nitroaromatic Explosives Decomposition. Small, 2020, 16, e1902944.	5.2	36
95	Functional 2D Germanene Fluorescent Coating of Microrobots for Micromachines Multiplexing. Small, 2020, 16, e1902365.	5.2	31
96	Fe(0)-embedded thermally reduced graphene oxide as efficient nanocatalyst for reduction of nitro compounds to amines. Chemical Engineering Journal, 2020, 382, 122469.	6.6	54
97	Graphitic nanofibers decorated with Ni3S2 interlaced nanosheets as efficient binder-free cathodes for hybrid supercapacitors. Applied Surface Science, 2020, 505, 143828.	3.1	10
98	Non-aqueous solution-processed phosphorene by controlled low-potential electrochemical exfoliation and thin film preparation. Nanoscale, 2020, 12, 2638-2647.	2.8	33
99	Black phosphorus–arsenic alloys for lithium ion batteries. FlatChem, 2020, 19, 100143.	2.8	22
100	Black arsenic: a new synthetic method by catalytic crystallization of arsenic glass. Nanoscale, 2020, 12, 5397-5401.	2.8	12
101	Hexagonal and Cubic Boron Nitride in Bulk and Nanosized Forms and Their Capacitive Behavior. ChemElectroChem, 2020, 7, 74-77.	1.7	6
102	Elements beyond graphene: Current state and perspectives of elemental monolayer deposition by bottom-up approach. Applied Materials Today, 2020, 18, 100502.	2.3	29
103	Layered black phosphorus as a reducing agent – decoration with group 10 elements. RSC Advances, 2020, 10, 36452-36458.	1.7	5
104	Enhanced voltammetric determination of metal ions by using a bismuthene-modified screen-printed electrode. Electrochimica Acta, 2020, 362, 137144.	2.6	25
105	Stabilization of Black Phosphorus by Sonicationâ€Assisted Simultaneous Exfoliation and Functionalization. Chemistry - A European Journal, 2020, 26, 17581-17587.	1.7	3
106	Recent Developments on the Single Atom Supported at 2D Materials Beyond Graphene as Catalysts. ACS Catalysis, 2020, 10, 9634-9648.	5.5	102
107	TaS <sub>2</sub> , TaSe <sub>2</sub> , and Their Heterogeneous Films as Catalysts for the Hydrogen Evolution Reaction. ACS Catalysis, 2020, 10, 3313-3325.	5.5	60
108	Boron and nitrogen dopants in graphene have opposite effects on the electrochemical detection of explosive nitroaromatic compounds. Electrochemistry Communications, 2020, 112, 106660.	2.3	15

#	Article	IF	CITATIONS
109	Potential Dependent Electrochemical Exfoliation of NiPS <sub>3</sub> and Implications for Hydrogen Evolution Reaction. ACS Applied Energy Materials, 2020, 3, 11992-11999.	2.5	19
110	Microwaveâ€Induced Structural Engineering and Pt Trapping in <i>6R</i> â€TaS <sub>2</sub> for the Hydrogen Evolution Reaction. Small, 2020, 16, e2003372.	5.2	18
111	A High-Performance Magnesium Triflate-based Electrolyte for Rechargeable Magnesium Batteries. Cell Reports Physical Science, 2020, 1, 100265.	2.8	48
112	MXene-Based Flexible Supercapacitors: Influence of an Organic Ionic Conductor Electrolyte on the Performance. ACS Applied Materials & amp; Interfaces, 2020, 12, 53039-53048.	4.0	42
113	Single-Step Synthesis of Platinoid-Decorated Phosphorene: Perspectives for Catalysis, Gas Sensing, and Energy Storage. ACS Applied Materials & Interfaces, 2020, 12, 50516-50526.	4.0	16
114	Liquid-Phase Exfoliated GeSe Nanoflakes for Photoelectrochemical-Type Photodetectors and Photoelectrochemical Water Splitting. ACS Applied Materials & Interfaces, 2020, 12, 48598-48613.	4.0	56
115	Integrated Biomonitoring Sensing with Wearable Asymmetric Supercapacitors Based on Ti <sub>3</sub> C <sub>2</sub> MXene and 1Tâ€Phase WS <sub>2</sub> Nanosheets. Advanced Functional Materials, 2020, 30, 2003673.	7.8	80
116	Structural Manipulation of Layered TiS <sub>2</sub> to TiS <sub>3</sub> Nanobelts through Niobium Doping for Highâ€Performance Supercapacitors. ChemElectroChem, 2020, 7, 4985-4989.	1.7	2
117	Polydimethylsiloxane–graphene oxide composite improving performance by ion beam irradiation. Surface and Interface Analysis, 2020, 52, 1156-1162.	0.8	8
118	Surface Energy of Black Phosphorus Alloys with Arsenic. ChemNanoMat, 2020, 6, 821-826.	1.5	6
119	Freestanding LiFe0.2Mn0.8PO4/rGO nanocomposites as high energy density fast charging cathodes for lithium-ion batteries. Materials Today Energy, 2020, 16, 100416.	2.5	8
120	Chemistry of Germanene: Surface Modification of Germanane Using Alkyl Halides. ACS Nano, 2020, 14, 7319-7327.	7.3	26
121	2D Germanane Derivative as a Vector for Overcoming Doxorubicin Resistance in Cancer Cells. Applied Materials Today, 2020, 20, 100697.	2.3	8
122	Surface Functionalization of 2D Transition Metal Oxides and Dichalcogenides via Covalent and Non-covalent Bonding for Sustainable Energy and Biomedical Applications. ACS Applied Nano Materials, 2020, 3, 3116-3143.	2.4	67
123	Acetonitrile-assisted exfoliation of layered grey and black arsenic: contrasting properties. Nanoscale Advances, 2020, 2, 1282-1289.	2.2	21
124	Tunable Roomâ€Temperature Synthesis of ReS <sub>2</sub> Bicatalyst on 3D―and 2Dâ€Printed Electrodes for Photo―and Electrochemical Energy Applications. Advanced Functional Materials, 2020, 30, 1910193.	7.8	45
125	Layered platinum dichalcogenides (PtS2, PtSe2, PtTe2) for non-enzymatic electrochemical sensor. Applied Materials Today, 2020, 19, 100606.	2.3	11
126	"Top-down―Arsenene Production by Low-Potential Electrochemical Exfoliation. Inorganic Chemistry, 2020, 59, 11259-11265.	1.9	23

#	Article	IF	CITATIONS
127	Comparison of GO and polymer microcapacitors prepared by ion beam writing. Surface and Interface Analysis, 2020, 52, 1171-1177.	0.8	1
128	Microcapacitors on graphene oxide and synthetic polymers prepared by microbeam lithography. Applied Surface Science, 2020, 528, 146802.	3.1	9
129	Smartdust 3Dâ€Printed Grapheneâ€Based Al/Ga Robots for Photocatalytic Degradation of Explosives. Small, 2020, 16, 2002111.	5.2	22
130	Graphene-Supported 2D transition metal dichalcogenide van der waals heterostructures. Applied Materials Today, 2020, 19, 100600.	2.3	64
131	Niobium-doped TiS2: Formation of TiS3 nanobelts and their effects in enzymatic biosensors. Biosensors and Bioelectronics, 2020, 155, 112114.	5.3	19
132	Molecular-Scale Characterization of Photoinduced Charge Separation in Mixed-Dimensional InSe–Organic van der Waals Heterostructures. ACS Nano, 2020, 14, 3509-3518.	7.3	17
133	Will Any Crap We Put into Graphene Increase Its Electrocatalytic Effect?. ACS Nano, 2020, 14, 21-25.	7.3	158
134	MXene Titanium Carbide-based Biosensor: Strong Dependence of Exfoliation Method on Performance. Analytical Chemistry, 2020, 92, 2452-2459.	3.2	155
135	Large-Scale Production of Nanocrystalline Black Phosphorus Ceramics. ACS Applied Materials & Interfaces, 2020, 12, 7381-7391.	4.0	23
136	Bipolar Electrochemistry Exfoliation of Layered Metal Chalcogenides Sb <sub>2</sub> S <sub>3</sub> and Bi <sub>2</sub> S <sub>3</sub> and their Hydrogen Evolution Applications. Chemistry - A European Journal, 2020, 26, 6479-6483.	1.7	15
137	Structural transition induced by niobium doping in layered titanium disulfide: The impact on electrocatalytic performance. Applied Materials Today, 2020, 19, 100555.	2.3	5
138	Solutionâ€Processed GaSe Nanoflakeâ€Based Films for Photoelectrochemical Water Splitting and Photoelectrochemicalâ€Type Photodetectors. Advanced Functional Materials, 2020, 30, 1909572.	7.8	81
139	Free tanding Black Phosphorus Foils for Energy Storage and Catalysis. Chemistry - A European Journal, 2020, 26, 8162-8169.	1.7	15
140	Emerging pnictogen-based 2D semiconductors: sensing and electronic devices. Nanoscale, 2020, 12, 10430-10446.	2.8	22
141	Autogenous Formation of Gold on Layered Black Phosphorus for Catalytic Purification of Waste Water. ACS Applied Materials & Interfaces, 2020, 12, 22702-22709.	4.0	11
142	Positive and Negative Effects of Dopants toward Electrocatalytic Activity of MoS <sub>2</sub> and WS <sub>2</sub> : Experiments and Theory. ACS Applied Materials & Interfaces, 2020, 12, 20383-20392.	4.0	38
143	Electrodeposited NiSe on a forest of carbon nanotubes as a free-standing electrode for hybrid supercapacitors and overall water splitting. Journal of Colloid and Interface Science, 2020, 574, 300-311.	5.0	83
144	Towards Antimonene and 2D Antimony Telluride through Electrochemical Exfoliation. Chemistry - A European Journal, 2020, 26, 6583-6590.	1.7	32

#	Article	IF	CITATIONS
145	Synthesis Protocols of the Most Common Layered Carbide and Nitride MAX Phases. Small Methods, 2020, 4, 1900780.	4.6	53
146	Nano-LED induced chemical reactions for structuring processes. Nanoscale Advances, 2020, 2, 5421-5427.	2.2	9
147	Spectroscopic thickness and quality metrics for PtSe <sub>2</sub> layers produced by top-down and bottom-up techniques. 2D Materials, 2020, 7, 045027.	2.0	21
148	Atomically Thin 2Dâ€Arsenene by Liquidâ€Phased Exfoliation: Toward Selective Vapor Sensing. Advanced Functional Materials, 2019, 29, 1807004.	7.8	80
149	Chemical bonding and thermodynamic properties of gallium and indium monochalcogenides. Journal of Chemical Thermodynamics, 2019, 128, 97-102.	1.0	6
150	Supercapacitors in Motion: Autonomous Microswimmers for Naturalâ€Resource Recovery. Angewandte Chemie - International Edition, 2019, 58, 13340-13344.	7.2	14
151	Supercapacitors in Motion: Autonomous Microswimmers for Naturalâ€Resource Recovery. Angewandte Chemie, 2019, 131, 13474-13478.	1.6	2
152	Germanane synthesis with simultaneous covalent functionalization: towards highly functionalized fluorescent germananes. Nanoscale, 2019, 11, 19327-19333.	2.8	17
153	Cloisite Microrobots as Self-Propelling Cleaners for Fast and Efficient Removal of Improvised Organophosphate Nerve Agents. ACS Applied Materials & Interfaces, 2019, 11, 31832-31843.	4.0	15
154	2D Stacks of MXene Ti <sub>3</sub> C <sub>2</sub> and 1Tâ€Phase WS <sub>2</sub> with Enhanced Capacitive Behavior. ChemElectroChem, 2019, 6, 3982-3986.	1.7	39
155	In Situ Doping of Black Phosphorus by High-Pressure Synthesis. Inorganic Chemistry, 2019, 58, 10227-10238.	1.9	20
156	Micromotors as "Motherships― A Concept for the Transport, Delivery, and Enzymatic Release of Molecular Cargo via Nanoparticles. Langmuir, 2019, 35, 10618-10624.	1.6	18
157	Beyond Graphene: Chemistry of Group 14 Graphene Analogues: Silicene, Germanene, and Stanene. ACS Nano, 2019, 13, 8566-8576.	7.3	93
158	Modification of MoS2 structure by means of high energy ions in connection to electrical properties and light element surface adsorption. Surfaces and Interfaces, 2019, 17, 100357.	1.5	9
159	Flexible freestanding MoS <sub>2</sub> -based composite paper for energy conversion and storage. Beilstein Journal of Nanotechnology, 2019, 10, 1488-1496.	1.5	8
160	Synthesis, Composition, and Properties of Partially Oxidized Graphite Oxides. Materials, 2019, 12, 2367.	1.3	10
161	Chalcogenide vacancies drive the electrocatalytic performance of rhenium dichalcogenides. Nanoscale, 2019, 11, 14684-14690.	2.8	15
162	Exfoliated transition metal dichalcogenide (MX2; M = Mo, W; X = S, Se, Te) nanosheets and their composites with polyaniline nanofibers for electrochemical capacitors. Applied Materials Today, 2019, 16, 280-289.	2.3	28

#	Article	IF	CITATIONS
163	Binary Phosphorene Redox Behavior in Oxidoreductase Enzymatic Systems. ACS Nano, 2019, 13, 13217-13224.	7.3	22
164	Noncovalent Functionalization of Pnictogen Surfaces: From Small Molecules to 2D Heterostructures. Small, 2019, 15, e1903495.	5.2	11
165	Radioactive Uranium Preconcentration <i>via</i> Self-Propelled Autonomous Microrobots Based on Metal–Organic Frameworks. ACS Nano, 2019, 13, 11477-11487.	7.3	90
166	Alkali Metal Arenides as a Universal Synthetic Tool for Layered 2D Germanene Modification. Angewandte Chemie, 2019, 131, 16669-16674.	1.6	0
167	Alkali Metal Arenides as a Universal Synthetic Tool for Layered 2D Germanene Modification. Angewandte Chemie - International Edition, 2019, 58, 16517-16522.	7.2	14
168	Antimony Chalcogenide van der Waals Nanostructures for Energy Conversion and Storage. ACS Sustainable Chemistry and Engineering, 2019, 7, 15790-15798.	3.2	24
169	Coordination chemistry of 2D and layered gray arsenic: photochemical functionalization with chromium hexacarbonyl. NPG Asia Materials, 2019, 11, .	3.8	10
170	2H and 2H/1T-Transition Metal Dichalcogenide Films Prepared via Powderless Gas Deposition for the Hydrogen Evolution Reaction. ACS Sustainable Chemistry and Engineering, 2019, 7, 16440-16449.	3.2	10
171	MAX and MAB Phases: Two-Dimensional Layered Carbide and Boride Nanomaterials for Electrochemical Applications. ACS Applied Nano Materials, 2019, 2, 6010-6021.	2.4	47
172	MnPS3 shows anticancer behaviour towards lung cancer cells. FlatChem, 2019, 18, 100134.	2.8	5
173	Localized deoxygenation of graphene oxide foil by ion microbeam writing. Vacuum, 2019, 163, 10-14.	1.6	12
174	Mix-and-Read No-Wash Fluorescence DNA Sensing System Using Graphene Oxide: Analytical Performance of Fresh Versus Aged Dispersions. ACS Omega, 2019, 4, 1611-1616.	1.6	4
175	Layered and two dimensional metal oxides for electrochemical energy conversion. Energy and Environmental Science, 2019, 12, 41-58.	15.6	310
176	Proteinase-sculptured 3D-printed graphene/polylactic acid electrodes as potential biosensing platforms: towards enzymatic modeling of 3D-printed structures. Nanoscale, 2019, 11, 12124-12131.	2.8	84
177	Lightâ€Driven Sandwich ZnO/TiO <sub>2</sub> /Pt Janus Micromotors: Schottky Barrier Suppression by Addition of TiO <sub>2</sub> Atomic Interface Layers into ZnO/Pt Micromachines Leading to Enhanced Fuelâ€Free Propulsion. Small Methods, 2019, 3, 1900258.	4.6	17
178	Flexible Pt/Graphene Foil Containing only 6.6 wt % of Pt has a Comparable Hydrogen Evolution Reaction Performance to Platinum Metal. ACS Sustainable Chemistry and Engineering, 2019, 7, 11721-11727.	3.2	8
179	Catalytic hydrogen evolution reaction on "metal-free―graphene: key role of metallic impurities. Nanoscale, 2019, 11, 11083-11085.	2.8	19
180	Edge vs. basal plane electrochemistry of layered pnictogens (As, Sb, Bi): Does edge always offer faster electron transfer?. Applied Materials Today, 2019, 16, 179-184.	2.3	8

#	Article	IF	CITATIONS
181	Equipartition of Energy Defines the Size–Thickness Relationship in Liquid-Exfoliated Nanosheets. ACS Nano, 2019, 13, 7050-7061.	7.3	123
182	Selenium covalently modified graphene: towards gas sensing. 2D Materials, 2019, 6, 034006.	2.0	4
183	Thiographene synthesized from fluorographene <i>via</i> xanthogenate with immobilized enzymes for environmental remediation. Nanoscale, 2019, 11, 10695-10701.	2.8	8
184	Electrochemistry of Layered Semiconducting A <sup>III</sup> B <sup>VI</sup> Chalcogenides: Indium Monochalcogenides (InS, InSe, InTe). ChemCatChem, 2019, 11, 2634-2642.	1.8	20
185	Layered Crystalline and Amorphous Platinum Disulfide (PtS <sub>2</sub> ): Contrasting Electrochemistry. Chemistry - A European Journal, 2019, 25, 7330-7338.	1.7	20
186	MoS <sub>2</sub> versatile spray-coating of 3D electrodes for the hydrogen evolution reaction. Nanoscale, 2019, 11, 9888-9895.	2.8	24
187	Atomic Layer Deposition as a General Method Turns any 3Dâ€Printed Electrode into a Desired Catalyst: Case Study in Photoelectrochemisty. Advanced Energy Materials, 2019, 9, 1900994.	10.2	28
188	Recyclable nanographene-based micromachines for the on-the-fly capture of nitroaromatic explosives. Nanoscale, 2019, 11, 8825-8834.	2.8	28
189	Chemistry of Layered Pnictogens: Phosphorus, Arsenic, Antimony, and Bismuth. Angewandte Chemie, 2019, 131, 7631-7637.	1.6	14
190	Effects of the ion bombardment on the structure and composition of GO and rGO foils. Materials Chemistry and Physics, 2019, 232, 272-277.	2.0	23
191	Chemistry of Layered Pnictogens: Phosphorus, Arsenic, Antimony, and Bismuth. Angewandte Chemie - International Edition, 2019, 58, 7551-7557.	7.2	48
192	Mildly oxidized SWCNT as new potential support membrane material for effective H2/CO2 separation. Applied Materials Today, 2019, 15, 335-342.	2.3	11
193	Fluorine saturation on thermally reduced graphene. Applied Materials Today, 2019, 15, 343-349.	2.3	8
194	Localized modification of graphene oxide properties by laser irradiation in vacuum. Vacuum, 2019, 165, 134-138.	1.6	25
195	Recoverable Bismuth-Based Microrobots: Capture, Transport, and On-Demand Release of Heavy Metals and an Anticancer Drug in Confined Spaces. ACS Applied Materials & Interfaces, 2019, 11, 13359-13369.	4.0	42
196	Catalytic and Lightâ€Ðriven ZnO/Pt Janus Nano/Micromotors: Switching of Motion Mechanism via Interface Roughness and Defect Tailoring at the Nanoscale. Advanced Functional Materials, 2019, 29, 1808678.	7.8	74
197	The capacitance and electron transfer of 3D-printed graphene electrodes are dramatically influenced by the type of solvent used for pre-treatment. Electrochemistry Communications, 2019, 102, 83-88.	2.3	96
198	Shear-force exfoliation of indium and gallium chalcogenides for selective gas sensing applications. Nanoscale, 2019, 11, 4310-4317.	2.8	28

#	Article	IF	CITATIONS
199	A Metalâ€Doped Fungiâ€Based Biomaterial for Advanced Electrocatalysis. Chemistry - A European Journal, 2019, 25, 3828-3834.	1.7	2
200	Exfoliation of Calcium Germanide by Alkyl Halides. Chemistry of Materials, 2019, 31, 10126-10134.	3.2	18
201	Interaction of single- and double-stranded DNA with multilayer MXene by fluorescence spectroscopy and molecular dynamics simulations. Chemical Science, 2019, 10, 10010-10017.	3.7	59
202	Niobium disulphide (NbS <sub>2</sub> )-based (heterogeneous) electrocatalysts for an efficient hydrogen evolution reaction. Journal of Materials Chemistry A, 2019, 7, 25593-25608.	5.2	50
203	The Structural and Compositional Changes of Graphene Oxide Induced by Irradiation With 500 keV Helium and Gallium Ions. Physica Status Solidi (B): Basic Research, 2019, 256, 1800409.	0.7	11
204	Pnictogenâ€Based Enzymatic Phenol Biosensors: Phosphorene, Arsenene, Antimonene, and Bismuthene. Angewandte Chemie - International Edition, 2019, 58, 134-138.	7.2	96
205	Exfoliated Layered Manganese Trichalcogenide Phosphite (MnP <i>X</i> <sub>3</sub> , <i>X</i> = S, Se) as Electrocatalytic van der Waals Materials for Hydrogen Evolution. Advanced Functional Materials, 2019, 29, 1805975.	7.8	85
206	Pnictogenâ€Based Enzymatic Phenol Biosensors: Phosphorene, Arsenene, Antimonene, and Bismuthene. Angewandte Chemie, 2019, 131, 140-144.	1.6	4
207	Tuning of electrocatalytic properties of MoS2 by chalcogenide ion implantation. Applied Materials Today, 2019, 14, 216-223.	2.3	18
208	Cytotoxicity of Shear Exfoliated Pnictogen (As, Sb, Bi) Nanosheets. Chemistry - A European Journal, 2019, 25, 2242-2249.	1.7	34
209	Ultrapure Graphene Is a Poor Electrocatalyst: Definitive Proof of the Key Role of Metallic Impurities in Graphene-Based Electrocatalysis. ACS Nano, 2019, 13, 1574-1582.	7.3	92
210	Hot Carrier and Surface Recombination Dynamics in Layered InSe Crystals. Journal of Physical Chemistry Letters, 2019, 10, 493-499.	2.1	22
211	Black Phosphorus Cytotoxicity Assessments Pitfalls: Advantages and Disadvantages of Metabolic and Morphological Assays. Chemistry - A European Journal, 2019, 25, 349-360.	1.7	18
212	Ultrafast Electrochemical Trigger Drug Delivery Mechanism for Nanographene Micromachines. Advanced Functional Materials, 2019, 29, 1806696.	7.8	78
213	Metal Phosphorous Trichalcogenides (MPCh <sub>3</sub> ): From Synthesis to Contemporary Energy Challenges. Angewandte Chemie - International Edition, 2019, 58, 9326-9337.	7.2	73
214	Metallâ€Phosphorâ€Trichalkogenide (MPCh 3 ): von der Synthese zu aktuellen Energieanwendungen. Angewandte Chemie, 2019, 131, 9426-9438.	1.6	5
215	In vitro cytotoxicity of covalently protected layered molybdenum disulfide. Applied Materials Today, 2018, 11, 200-206.	2.3	19
216	Frontispiece: Chemistry of Graphene Derivatives: Synthesis, Applications, and Perspectives. Chemistry - A European Journal, 2018, 24, .	1.7	0

#	Article	IF	CITATIONS
217	The chemistry of CVD graphene. Journal of Materials Chemistry C, 2018, 6, 6082-6101.	2.7	95
218	3D-Printed Graphene/Polylactic Acid Electrodes Promise High Sensitivity in Electroanalysis. Analytical Chemistry, 2018, 90, 5753-5757.	3.2	205
219	Hydrogenation of Fluorographite and Fluorographene: An Easy Way to Produce Highly Hydrogenated Graphene. Chemistry - A European Journal, 2018, 24, 8350-8360.	1.7	6
220	Graphene oxide layers modified by irradiation with 1.2â€⁻MeV He+ ions. Surface and Coatings Technology, 2018, 342, 220-225.	2.2	22
221	Nonconductive layered hexagonal boron nitride exfoliation by bipolar electrochemistry. Nanoscale, 2018, 10, 7298-7303.	2.8	51
222	Cation-Controlled Electrocatalytical Activity of Transition-Metal Disulfides. ACS Catalysis, 2018, 8, 2774-2781.	5.5	58
223	Black Phosphorus Synthesis Path Strongly Influences Its Delamination, Chemical Properties and Electrochemical Performance. ACS Applied Energy Materials, 2018, 1, 503-509.	2.5	19
224	A simplified protocol for the usage of new immuno-SERS probes for the detection of casein, collagens and ovalbumin in the cross-sections of artworks. Analytical Methods, 2018, 10, 1054-1062.	1.3	3
225	Morphological Effects and Stabilization of the Metallic 1T Phase in Layered Vâ€, Nbâ€, and Taâ€Đoped WSe <sub>2</sub> for Electrocatalysis. Chemistry - A European Journal, 2018, 24, 3199-3208.	1.7	38
226	Metallic impurities in black phosphorus nanoflakes prepared by different synthetic routes. Nanoscale, 2018, 10, 1540-1546.	2.8	29
227	MoS <sub>2</sub> Nanoparticles as Electrocatalytic Labels in Magneto-Immunoassays. ACS Applied Materials & Interfaces, 2018, 10, 16861-16866.	4.0	11
228	Layered PtTe <sub>2</sub> Matches Electrocatalytic Performance of Pt/C for Oxygen Reduction Reaction with Significantly Lower Toxicity. ACS Sustainable Chemistry and Engineering, 2018, 6, 7432-7441.	3.2	56
229	Making Ultrafast High apacity Anodes for Lithiumâ€Ion Batteries via Antimony Doping of Nanosized Tin Oxide/Graphene Composites. Advanced Functional Materials, 2018, 28, 1706529.	7.8	31
230	Chemistry of Graphene Derivatives: Synthesis, Applications, and Perspectives. Chemistry - A European Journal, 2018, 24, 5992-6006.	1.7	99
231	Cytotoxicity of Group 5 Transition Metal Ditellurides (MTe <sub>2</sub> ; M=V, Nb, Ta). Chemistry - A European Journal, 2018, 24, 206-211.	1.7	32
232	TaS <sub>3</sub> Nanofibers: Layered Trichalcogenide for High-Performance Electronic and Sensing Devices. ACS Nano, 2018, 12, 464-473.	7.3	30
233	One‣tep Synthesis of B/N Coâ€doped Graphene as Highly Efficient Electrocatalyst for the Oxygen Reduction Reaction: Synergistic Effect of Impurities. Chemistry - A European Journal, 2018, 24, 928-936.	1.7	26
234	WSe <sub>2</sub> nanoparticles with enhanced hydrogen evolution reaction prepared by bipolar electrochemistry: application in competitive magneto-immunoassay. Nanoscale, 2018, 10, 23149-23156.	2.8	24

#	Article	IF	CITATIONS
235	Reprint of "Graphene oxide layers modified by irradiation with 1.2â€⁻MeV He+ ions― Surface and Coatings Technology, 2018, 355, 301-306.	2.2	1
236	3D Printed Graphene Electrodes' Electrochemical Activation. ACS Applied Materials & Interfaces, 2018, 10, 40294-40301.	4.0	188
237	Cytotoxicity of layered metal phosphorus chalcogenides (MPXY) nanoflakes; FePS3, CoPS3, NiPS3. FlatChem, 2018, 12, 1-9.	2.8	24
238	Fluorographenes for Energy and Sensing Application: The Amount of Fluorine Matters. ACS Omega, 2018, 3, 17700-17706.	1.6	6
239	Metal-Free Visible-Light Photoactivated C <sub>3</sub> N <sub>4</sub> Bubble-Propelled Tubular Micromotors with Inherent Fluorescence and On/Off Capabilities. ACS Nano, 2018, 12, 12482-12491.	7.3	85
240	ZnO/ZnO <sub>2</sub> /Pt Janus Micromotors Propulsion Mode Changes with Size and Interface Structure: Enhanced Nitroaromatic Explosives Degradation under Visible Light. ACS Applied Materials & Interfaces, 2018, 10, 42688-42697.	4.0	70
241	1T-Phase Tungsten Chalcogenides (WS <sub>2</sub> , WSe <sub>2</sub> , WTe <sub>2</sub> ) Decorated with TiO <sub>2</sub> Nanoplatelets with Enhanced Electron Transfer Activity for Biosensing Applications. ACS Applied Nano Materials, 2018, 1, 7006-7015.	2.4	32
242	Cytotoxicity of phosphorus allotropes (black, violet, red). Applied Materials Today, 2018, 13, 310-319.	2.3	23
243	Cooperative Multifunctional Selfâ€Propelled Paramagnetic Microrobots with Chemical Handles for Cell Manipulation and Drug Delivery. Advanced Functional Materials, 2018, 28, 1804343.	7.8	81
244	Covalent Functionalization of Exfoliated Arsenic with Chlorocarbene. Angewandte Chemie, 2018, 130, 15053-15056.	1.6	4
245	Graphite oxide based targets applied in laser matter interaction. EPJ Web of Conferences, 2018, 167, 02004.	0.1	11
246	Laser modification of graphene oxide layers. EPJ Web of Conferences, 2018, 167, 04010.	0.1	8
247	Covalent Functionalization of Exfoliated Arsenic with Chlorocarbene. Angewandte Chemie - International Edition, 2018, 57, 14837-14840.	7.2	23
248	Triazine- and Heptazine-Based Carbon Nitrides: Toxicity. ACS Applied Nano Materials, 2018, 1, 4442-4449.	2.4	41
249	Graphene oxide layers modified by irradiation with 1.0 MeV Au <sup>+</sup> ions. Surface and Interface Analysis, 2018, 50, 1110-1115.	0.8	12
250	A highly sensitive room temperature humidity sensor based on 2D-WS2 nanosheets. FlatChem, 2018, 9, 21-26.	2.8	30
251	Investigation of electrocatalytic activity on a N-doped reduced graphene oxide surface for the oxygen reduction reaction in an alkaline medium. International Journal of Hydrogen Energy, 2018, 43, 12129-12139.	3.8	33
252	MoSe <sub>2</sub> Dispersed in Stabilizing Surfactant Media: Effect of the Surfactant Type and Concentration on Electron Transfer and Catalytic Properties. ACS Applied Materials & Interfaces, 2018, 10, 17820-17826.	4.0	25

#	Article	IF	CITATIONS
253	Phase Transformation Induced Self-Healing Behavior of Al-Ag Alloy. Materials, 2018, 11, 199.	1.3	7
254	Fluorination of Black Phosphorus—Will Black Phosphorus Burn Down in the Elemental Fluorine?. Advanced Functional Materials, 2018, 28, 1801438.	7.8	34
255	Synthesis and properties of phosphorus and sulfur co-doped graphene. New Journal of Chemistry, 2018, 42, 16093-16102.	1.4	6
256	Unique wettability phenomenon of carbon-bonded alumina with advanced nanocoating. Applied Materials Today, 2018, 13, 24-31.	2.3	11
257	Products of Degradation of Black Phosphorus in Protic Solvents. ACS Nano, 2018, 12, 8390-8396.	7.3	70
258	Layered franckeite and teallite intrinsic heterostructures: shear exfoliation and electrocatalysis. Journal of Materials Chemistry A, 2018, 6, 16590-16599.	5.2	18
259	Fluorographene and Graphane as an Excellent Platform for Enzyme Biocatalysis. Chemistry - A European Journal, 2018, 24, 16833-16839.	1.7	8
260	Solutionâ€Based Processing of Optoelectronically Active Indium Selenide. Advanced Materials, 2018, 30, e1802990.	11.1	78
261	Functional Protection of Exfoliated Black Phosphorus by Noncovalent Modification with Anthraquinone. ACS Nano, 2018, 12, 5666-5673.	7.3	79
262	Electrochemistry of layered metal diborides. Nanoscale, 2018, 10, 11544-11552.	2.8	40
263	Schwarzer Phosphor neu entdeckt: vom Volumenmaterial zu Monoschichten. Angewandte Chemie, 2017, 129, 8164-8185.	1.6	59
264	Black Phosphorus Rediscovered: From Bulk Material to Monolayers. Angewandte Chemie - International Edition, 2017, 56, 8052-8072.	7.2	407
265	Doping with Graphitic Nitrogen Triggers Ferromagnetism in Graphene. Journal of the American Chemical Society, 2017, 139, 3171-3180.	6.6	202
266	A study of the effect of sonication time on the catalytic performance of layered WS <sub>2</sub> from various sources. Physical Chemistry Chemical Physics, 2017, 19, 2768-2777.	1.3	5
267	Structural and optical properties of vanadium ion-implanted GaN. Nuclear Instruments & Methods in Physics Research B, 2017, 406, 53-57.	0.6	2
268	Black phosphorus nanoparticles as a novel fluorescent sensing platform for nucleic acid detection. Materials Chemistry Frontiers, 2017, 1, 1130-1136.	3.2	82
269	Synthesis of Carboxylated-Graphenes by the Kolbe–Schmitt Process. ACS Nano, 2017, 11, 1789-1797.	7.3	45
270	Functional Nanosheet Synthons by Covalent Modification of Transition-Metal Dichalcogenides. Chemistry of Materials, 2017, 29, 2066-2073.	3.2	56

#	Article	IF	CITATIONS
271	Investigation on the ability of heteroatom-doped graphene for biorecognition. Nanoscale, 2017, 9, 3530-3536.	2.8	8
272	The stopping power and energy straggling of light ions in graphene oxide foils. Nuclear Instruments & Methods in Physics Research B, 2017, 406, 173-178.	0.6	8
273	Concentration of Nitric Acid Strongly Influences Chemical Composition of Graphite Oxide. Chemistry - A European Journal, 2017, 23, 6432-6440.	1.7	24
274	3R phase of MoS <sub>2</sub> and WS <sub>2</sub> outperforms the corresponding 2H phase for hydrogen evolution. Chemical Communications, 2017, 53, 3054-3057.	2.2	180
275	2D Monoelemental Arsenene, Antimonene, and Bismuthene: Beyond Black Phosphorus. Advanced Materials, 2017, 29, 1605299.	11.1	601
276	Near‣toichiometric Bulk Graphane from Halogenated Graphenes (X = Cl/Br/I) by the Birch Reduction for High Density Energy Storage. Advanced Functional Materials, 2017, 27, 1605797.	7.8	20
277	Group 6 Layered Transition-Metal Dichalcogenides in Lab-on-a-Chip Devices: 1T-Phase WS <sub>2</sub> for Microfluidics Non-Enzymatic Detection of Hydrogen Peroxide. Analytical Chemistry, 2017, 89, 4978-4985.	3.2	34
278	2H→1T Phase Engineering of Layered Tantalum Disulfides in Electrocatalysis: Oxygen Reduction Reaction. Chemistry - A European Journal, 2017, 23, 8082-8091.	1.7	33
279	Facile synthesis of magnetic Co nanofoam by lowâ€ŧemperature thermal decomposition of Co glycerolate. Micro and Nano Letters, 2017, 12, 278-280.	0.6	6
280	The Covalent Functionalization of Layered Black Phosphorus by Nucleophilic Reagents. Angewandte Chemie - International Edition, 2017, 56, 9891-9896.	7.2	159
281	Towards stoichiometric analogues of graphene: graphane, fluorographene, graphol, graphene acid and others. Chemical Society Reviews, 2017, 46, 4450-4463.	18.7	83
282	Universal Method for Large‧cale Synthesis of Layered Transition Metal Dichalcogenides. Chemistry - A European Journal, 2017, 23, 10177-10186.	1.7	22
283	Planar Polyolefin Nanostripes: Perhydrogenated Graphene. Chemistry - A European Journal, 2017, 23, 11961-11968.	1.7	4
284	Two-Dimensional 1T-Phase Transition Metal Dichalcogenides as Nanocarriers To Enhance and Stabilize Enzyme Activity for Electrochemical Pesticide Detection. ACS Nano, 2017, 11, 5774-5784.	7.3	109
285	Nitrogen-doped graphene: effect of graphite oxide precursors and nitrogen content on the electrochemical sensing properties. Physical Chemistry Chemical Physics, 2017, 19, 15914-15923.	1.3	33
286	Selective Bromination of Graphene Oxide by the Hunsdiecker Reaction. Chemistry - A European Journal, 2017, 23, 10473-10479.	1.7	21
287	Low-Temperature PM IRRAS of a Monolayer on Au: Spectra of C <sub>18</sub> D <sub>37</sub> SH. Langmuir, 2017, 33, 5613-5616.	1.6	1
288	Thin, Highâ€Flux, Selfâ€Standing, Graphene Oxide Membranes for Efficient Hydrogen Separation from Gas Mixtures. Chemistry - A European Journal, 2017, 23, 11416-11422.	1.7	26

#	Article	IF	CITATIONS
289	Graphene/Group 5 Transition Metal Dichalcogenide Composites for Electrochemical Applications. Chemistry - A European Journal, 2017, 23, 10430-10437.	1.7	10
290	Graphene oxide layers modified by light energetic ions. Physical Chemistry Chemical Physics, 2017, 19, 10282-10291.	1.3	49
291	Layered Metal Thiophosphite Materials: Magnetic, Electrochemical, and Electronic Properties. ACS Applied Materials & Interfaces, 2017, 9, 12563-12573.	4.0	179
292	Coke-derived graphene quantum dots as fluorescence nanoquencher in DNA detection. Applied Materials Today, 2017, 7, 138-143.	2.3	51
293	Efficient heat dissipation in AlGaN/GaN heterostructure grown on silver substrate. Applied Materials Today, 2017, 7, 134-137.	2.3	28
294	The Origin of MoS <sub>2</sub> Significantly Influences Its Performance for the Hydrogen Evolution Reaction due to Differences in Phase Purity. Chemistry - A European Journal, 2017, 23, 3169-3177.	1.7	20
295	1Tâ€Phase WS <sub>2</sub> Proteinâ€Based Biosensor. Advanced Functional Materials, 2017, 27, 1604923.	7.8	43
296	Tuning of graphene oxide composition by multiple oxidations for carbon dioxide storage and capture of toxic metals. Journal of Materials Chemistry A, 2017, 5, 2739-2748.	5.2	87
297	Ultrapure Molybdenum Disulfide Shows Enhanced Catalysis for Hydrogen Evolution over Impuritiesâ€Đoped Counterpart. ChemCatChem, 2017, 9, 1168-1171.	1.8	16
298	Fast Synthesis of Highly Oxidized Graphene Oxide. ChemistrySelect, 2017, 2, 9000-9006.	0.7	29
299	The Role of the Metal Element in Layered Metal Phosphorus Triselenides upon Their Electrochemical Sensing and Energy Applications. ACS Catalysis, 2017, 7, 8159-8170.	5.5	83
300	Thermodynamic properties of misfit cobaltite [Bi2-xCa2O4][CoO2]1.7. Thermochimica Acta, 2017, 656, 129-134.	1.2	4
301	Black-phosphorus-enhanced bubble-propelled autonomous catalytic microjets. Applied Materials Today, 2017, 9, 289-291.	2.3	20
302	Thermal properties of graphite oxide, thermally reduced graphene and chemically reduced graphene. AIP Conference Proceedings, 2017, , .	0.3	5
303	Synergetic Metals on Carbocatalyst Shungite. Chemistry - A European Journal, 2017, 23, 18232-18238.	1.7	12
304	Black Phosphorus Nanoflakes/Polyaniline Hybrid Material for High-Performance Pseudocapacitors. Journal of Physical Chemistry C, 2017, 121, 20532-20538.	1.5	85
305	Layered Noble Metal Dichalcogenides: Tailoring Electrochemical and Catalytic Properties. ACS Applied Materials & Interfaces, 2017, 9, 25587-25599.	4.0	51
306	Structural and optical properties of Gd implanted GaN with various crystallographic orientations. Thin Solid Films, 2017, 638, 63-72.	0.8	13

#	Article	IF	CITATIONS
307	Pnictogen (As, Sb, Bi) Nanosheets for Electrochemical Applications Are Produced by Shear Exfoliation Using Kitchen Blenders. Angewandte Chemie - International Edition, 2017, 56, 14417-14422.	7.2	216
308	Pnictogen (As, Sb, Bi) Nanosheets for Electrochemical Applications Are Produced by Shear Exfoliation Using Kitchen Blenders. Angewandte Chemie, 2017, 129, 14609-14614.	1.6	87
309	2H → 1T Phase Change in Direct Synthesis of WS <sub>2</sub> Nanosheets via Solution-Based Electrochemical Exfoliation and Their Catalytic Properties. ACS Applied Materials & Interfaces, 2017, 9, 26350-26356.	4.0	61
310	Black Phosphorus Nanoparticles Potentiate the Anticancer Effect of Oxaliplatin in Ovarian Cancer Cell Line. Advanced Functional Materials, 2017, 27, 1701955.	7.8	51
311	Unconventionally Layered CoTe <sub>2</sub> and NiTe <sub>2</sub> as Electrocatalysts for Hydrogen Evolution. Chemistry - A European Journal, 2017, 23, 11719-11726.	1.7	76
312	Microwave irradiated N- and B,Cl-doped graphene: Oxidation method has strong influence on capacitive behavior. Applied Materials Today, 2017, 9, 204-211.	2.3	25
313	Introduction of sulfur to graphene oxide by Friedel-Crafts reaction. FlatChem, 2017, 6, 28-36.	2.8	7
314	1T-Phase Transition Metal Dichalcogenides (MoS <sub>2</sub> , MoSe <sub>2</sub> , WS <sub>2</sub> ,) Tj ETQq Enzyme-Based Biosensor. ACS Applied Materials & Interfaces, 2017, 9, 40697-40706.	0 0 0 rgBT 4.0	Överlock 1 138
315	Surface properties of MoS <sub>2</sub> probed by inverse gas chromatography and their impact on electrocatalytic properties. Nanoscale, 2017, 9, 19236-19244.	2.8	19
316	Innentitelbild: Pnictogen (As, Sb, Bi) Nanosheets for Electrochemical Applications Are Produced by Shear Exfoliation Using Kitchen Blenders (Angew. Chem. 46/2017). Angewandte Chemie, 2017, 129, 14510-14510.	1.6	2
317	Electrochemical Exfoliation of Layered Black Phosphorus into Phosphorene. Angewandte Chemie, 2017, 129, 10579-10581.	1.6	56
318	The Covalent Functionalization of Layered Black Phosphorus by Nucleophilic Reagents. Angewandte Chemie, 2017, 129, 10023-10028.	1.6	26
319	Electrochemical Exfoliation of Layered Black Phosphorus into Phosphorene. Angewandte Chemie - International Edition, 2017, 56, 10443-10445.	7.2	228
320	Layered Transition-Metal Ditellurides in Electrocatalytic Applications—Contrasting Properties. ACS Catalysis, 2017, 7, 5706-5716.	5.5	50
321	Cytotoxicity of Exfoliated Layered Vanadium Dichalcogenides. Chemistry - A European Journal, 2017, 23, 684-690.	1.7	38
322	Boron and Nitrogen Doped Graphene <i>via</i> Microwave Exfoliation for Simultaneous Electrochemical Detection of Ascorbic Acid, Dopamine and Uric Acid. Electroanalysis, 2017, 29, 45-50.	1.5	16
323	Graphitic carbon nitride: Effects of various precursors on the structural, morphological and electrochemical sensing properties. Applied Materials Today, 2017, 8, 150-162.	2.3	56
324	Fluorographene Modified by Grignard Reagents: A Broad Range of Functional Nanomaterials. Chemistry - A European Journal, 2017, 23, 1956-1964.	1.7	30

1

#	ARTICLE	IF	CITATIONS
325	GO/2D WS2 Based Humidity Sensor. Proceedings (mdpi), 2017, 1, 469.	0.2	2
326	Selfâ€Propelled Supercapacitors for Onâ€Demand Circuit Configuration Based on WS <sub>2</sub> Nanoparticles Micromachines. Advanced Functional Materials, 2016, 26, 6662-6667.	7.8	70
327	Layered Black Phosphorus: Strongly Anisotropic Magnetic, Electronic, and Electronâ€Transfer Properties. Angewandte Chemie, 2016, 128, 3443-3447.	1.6	27
328	Layered Platinum Dichalcogenides (PtS <sub>2</sub> , PtSe <sub>2</sub> , and PtTe <sub>2</sub> ) Electrocatalysis: Monotonic Dependence on the Chalcogen Size. Advanced Functional Materials, 2016, 26, 4306-4318.	7.8	228
329	Impact Electrochemistry: Detection of Graphene Nanosheets Labeled with Metal Nanoparticles through Oxygen Reduction Mediation. ChemPhysChem, 2016, 17, 2096-2099.	1.0	18
330	Layered Black Phosphorus: Strongly Anisotropic Magnetic, Electronic, and Electronâ€Transfer Properties. Angewandte Chemie - International Edition, 2016, 55, 3382-3386.	7.2	139
331	Contrasts between Mild and Harsh Oxidation of Carbon Nanotubes in terms of their Properties and Electrochemical Performance. ChemElectroChem, 2016, 3, 1713-1719.	1.7	11
332	Toward graphene chloride: chlorination of graphene and graphene oxide. RSC Advances, 2016, 6, 66884-66892.	1.7	56
333	Partially Hydrogenated Graphene Materials Exhibit High Electrocatalytic Activities Related to Unintentional Doping with Metallic Impurities. Chemistry - A European Journal, 2016, 22, 8627-8634.	1.7	11
334	Sulfur Doping Induces Strong Ferromagnetic Ordering in Graphene: Effect of Concentration and Substitution Mechanism. Advanced Materials, 2016, 28, 5045-5053.	11.1	94
335	Highly reliable long-term operation of AlGaN/GaN/AlN HFETs grown on silver substrate. , 2016, , .		0
336	Fabrication of UV sources for novel lithographical techniques: Development of nano-LED etching procedures. , 2016, , .		0
337	Exfoliation of Layered Topological Insulators Bi <sub>2</sub> Se <sub>3</sub> and Bi <sub>2</sub> Te <sub>3</sub> <i>via</i> Electrochemistry. ACS Nano, 2016, 10, 11442-11448.	7.3	97
338	Direct electro-optical pumping for hybrid CdSe nanocrystal/III-nitride based nano-light-emitting diodes. Applied Physics Letters, 2016, 108, 061107.	1.5	38
339	Doped Graphene for DNA Analysis: the Electrochemical Signal is Strongly Influenced by the Kind of Dopant and the Nucleobase Structure. Scientific Reports, 2016, 6, 33046.	1.6	25
340	Ferromagnetism: Sulfur Doping Induces Strong Ferromagnetic Ordering in Graphene: Effect of Concentration and Substitution Mechanism (Adv. Mater. 25/2016). Advanced Materials, 2016, 28, 5139-5139.	11.1	5
341	Hybrid optoelectronics based on a nanocrystal/III-N nano-LED platform. , 2016, , .		6

InGaN mesoscopic structures for low energy consumption nano-opto-electronics. , 2016, , .

#	Article	IF	CITATIONS
343	The structural and optical properties of metal ion-implanted GaN. Nuclear Instruments & Methods in Physics Research B, 2016, 371, 254-257.	0.6	6
344	Graphane Nanostripes. Angewandte Chemie, 2016, 128, 14171-14175.	1.6	7
345	Graphane Nanostripes. Angewandte Chemie - International Edition, 2016, 55, 13965-13969.	7.2	10
346	Electrocatalysis of layered Group 5 metallic transition metal dichalcogenides (MX <sub>2</sub> , M =) Tj ETQq0 (	0 0 <sub>5</sub> 28T /0	Overlock 10 T 218
347	Synthesis, structure, thermal, transport and magnetic properties of VN ceramics. Ceramics International, 2016, 42, 18779-18784.	2.3	16
348	Layered SnS versus SnS <sub>2</sub> : Valence and Structural Implications on Electrochemistry and Clean Energy Electrocatalysis. Journal of Physical Chemistry C, 2016, 120, 24098-24111.	1.5	85
349	Graphene Oxide Sorption Capacity toward Elements over the Whole Periodic Table: A Comparative Study. Journal of Physical Chemistry C, 2016, 120, 24203-24212.	1.5	56
350	Reducing emission of carcinogenic by-products in the production of thermally reduced graphene oxide. Green Chemistry, 2016, 18, 6618-6629.	4.6	11
351	Black Phosphorus Nanoparticle Labels for Immunoassays via Hydrogen Evolution Reaction Mediation. Analytical Chemistry, 2016, 88, 10074-10079.	3.2	142
352	Negative Electrocatalytic Effects of p-Doping Niobium and Tantalum on MoS <sub>2</sub> and WS <sub>2</sub> for the Hydrogen Evolution Reaction and Oxygen Reduction Reaction. ACS Catalysis, 2016, 6, 5724-5734.	5.5	174
353	Functionalization of Hydrogenated Graphene: Transitionâ€Metalâ€Catalyzed Crossâ€Coupling Reactions of Allylic Câ^'H Bonds. Angewandte Chemie, 2016, 128, 10909-10912.	1.6	12
354	Functionalization of Hydrogenated Graphene: Transitionâ€Metalâ€Catalyzed Crossâ€Coupling Reactions of Allylic Câ^'H Bonds. Angewandte Chemie - International Edition, 2016, 55, 10751-10754.	7.2	22
355	MoS <sub>2</sub> /WS <sub>2</sub> â€Graphene Composites through Thermal Decomposition of Tetrathiomolybdate/Tetrathiotungstate for Proton/Oxygen Electroreduction. ChemPhysChem, 2016, 17, 2890-2896.	1.0	12
356	MoSe <sub>2</sub> Nanolabels for Electrochemical Immunoassays. Analytical Chemistry, 2016, 88, 12204-12209.	3.2	33
357	Phosphorus and Halogen Coâ€Doped Graphene Materials and their Electrochemistry. Chemistry - A European Journal, 2016, 22, 15444-15450.	1.7	22
358	Valence and oxide impurities in MoS <sub>2</sub> and WS <sub>2</sub> dramatically change their electrocatalytic activity towards proton reduction. Nanoscale, 2016, 8, 16752-16760.	2.8	42
359	Synthesis of Graphene Oxide by Oxidation of Graphite with Ferrate(VI) Compounds: Myth or Reality?. Angewandte Chemie, 2016, 128, 12144-12148.	1.6	23
360	Synthesis of Graphene Oxide by Oxidation of Graphite with Ferrate(VI) Compounds: Myth or Reality?. Angewandte Chemie - International Edition, 2016, 55, 11965-11969.	7.2	25

#	Article	IF	CITATIONS
361	Synthesis procedure and type of graphite oxide strongly influence resulting graphene properties. Applied Materials Today, 2016, 4, 45-53.	2.3	87
362	Lipase enzymes on graphene oxide support for high-efficiency biocatalysis. Applied Materials Today, 2016, 5, 200-208.	2.3	26
363	Layered Postâ€Transitionâ€Metal Dichalcogenides (Xâ^'Mâ^'Mâ^'X) and Their Properties. Chemistry - A European Journal, 2016, 22, 18810-18816.	1.7	29
364	Microwave Exfoliation of Graphite Oxides in H <sub>2</sub> S Plasma for the Synthesis of Sulfur-Doped Graphenes as Oxygen Reduction Catalysts. ACS Applied Materials & Interfaces, 2016, 8, 31849-31855.	4.0	39
365	Catalytic properties of group 4 transition metal dichalcogenides (MX <sub>2</sub> ; M = Ti, Zr, Hf; X =) Tj ETQq1	l 0.78431 5.2	4 <sub>.7g</sub> BT /Ove
366	Doped and undoped graphene platforms: the influence of structural properties on the detection of polyphenols. Scientific Reports, 2016, 6, 20673.	1.6	12
367	A New Member of the Graphene Family: Graphene Acid. Chemistry - A European Journal, 2016, 22, 17416-17424.	1.7	44
368	Lithium Exfoliated Vanadium Dichalcogenides (VS <sub>2</sub> , VSe <sub>2</sub> , VTe <sub>2</sub> ) Exhibit Dramatically Different Properties from Their Bulk Counterparts. Advanced Materials Interfaces, 2016, 3, 1600433.	1.9	89
369	Simple Synthesis of Fluorinated Graphene: Thermal Exfoliation of Fluorographite. Chemistry - A European Journal, 2016, 22, 17696-17703.	1.7	26
370	Bipolar Electrochemical Synthesis of WS <sub>2</sub> Nanoparticles and Their Application in Magnetoâ€Immunosandwich Assay. Advanced Functional Materials, 2016, 26, 4094-4098.	7.8	43
371	Graphene–Amorphous Transitionâ€Metal Chalcogenide (MoS <sub><i>x</i></sub> ,) Tj ETQq1 1 0.784314 rgBT Evolution Reaction. ChemElectroChem, 2016, 3, 565-571.	/Overlock 1.7	2 10 Tf 50 3 41
372	Ball-milled sulfur-doped graphene materials contain metallic impurities originating from ball-milling apparatus: their influence on the catalytic properties. Physical Chemistry Chemical Physics, 2016, 18, 17875-17880.	1.3	42
373	Aromatic-Exfoliated Transition Metal Dichalcogenides: Implications for Inherent Electrochemistry and Hydrogen Evolution. ACS Catalysis, 2016, 6, 4594-4607.	5.5	80
374	Carboxylic Carbon Quantum Dots as a Fluorescent Sensing Platform for DNA Detection. ACS Applied Materials & Interfaces, 2016, 8, 1951-1957.	4.0	261
375	Fine tuning of graphene properties by modification with aryl halogens. Nanoscale, 2016, 8, 1493-1502.	2.8	21
376	Layered rhenium sulfide on free-standing three-dimensional electrodes is highly catalytic for the hydrogen evolution reaction: Experimental and theoretical study. Electrochemistry Communications, 2016, 63, 39-43.	2.3	54
377	Anti-MoS <sub>2</sub> Nanostructures: Tl <sub>2</sub> S and Its Electrochemical and Electronic Properties. ACS Nano, 2016, 10, 112-123.	7.3	18
378	Nanosized graphane (C <sub>1</sub> H <sub>1.14</sub> ) <sub>n</sub> by hydrogenation of carbon nanofibers by Birch reduction method. RSC Advances, 2016, 6, 6475-6485.	1.7	30

#	Article	IF	CITATIONS
379	Synthesis of spherical amorphous selenium nano and microparticles with tunable sizes. Micro and Nano Letters, 2016, 11, 91-93.	0.6	17
380	Multifunctional electrocatalytic hybrid carbon nanocables with highly active edges on their walls. Nanoscale, 2016, 8, 6700-6711.	2.8	10
381	Few-layer black phosphorus nanoparticles. Chemical Communications, 2016, 52, 1563-1566.	2.2	120
382	Electrochemistry of layered GaSe and GeS: applications to ORR, OER and HER. Physical Chemistry Chemical Physics, 2016, 18, 1699-1711.	1.3	77
383	Origin of exotic ferromagnetic behavior in exfoliated layered transition metal dichalcogenides MoS <sub>2</sub> and WS <sub>2</sub> . Nanoscale, 2016, 8, 1960-1967.	2.8	56
384	Layered Black Phosphorus as a Selective Vapor Sensor. Angewandte Chemie - International Edition, 2015, 54, 14317-14320.	7.2	187
385	Voltammetry of Layered Black Phosphorus: Electrochemistry of Multilayer Phosphorene. ChemElectroChem, 2015, 2, 295-295.	1.7	Ο
386	Selective Nitrogen Functionalization of Graphene by Bucherer-Type Reaction. Chemistry - A European Journal, 2015, 21, 7969-7969.	1.7	1
387	Metallic 1Tâ€WS <sub>2</sub> for Selective Impedimetric Vapor Sensing. Advanced Functional Materials, 2015, 25, 5611-5616.	7.8	122
388	Selective Nitrogen Functionalization of Graphene by Buchererâ€Type Reaction. Chemistry - A European Journal, 2015, 21, 8090-8095.	1.7	19
389	The Cytotoxicity of Layered Black Phosphorus. Chemistry - A European Journal, 2015, 21, 13991-13995.	1.7	173
390	Mesomeric Effects of Graphene Modified with Diazonium Salts: Substituent Type and Position Influence its Properties. Chemistry - A European Journal, 2015, 21, 17728-17738.	1.7	26
391	Transition Metal Oxides for the Oxygen Reduction Reaction: Influence of the Oxidation States of the Metal and its Position on the Periodic Table. ChemPhysChem, 2015, 16, 3527-3531.	1.0	47
392	Fluorinated Nanocarbons Cytotoxicity. Chemistry - A European Journal, 2015, 21, 13020-13026.	1.7	10
393	Pristine Basal―and Edgeâ€Planeâ€Oriented Molybdenite MoS <sub>2</sub> Exhibiting Highly Anisotropic Properties. Chemistry - A European Journal, 2015, 21, 7170-7178.	1.7	133
394	Ternary Transition Metal Oxide Nanoparticles with Spinel Structure for the Oxygen Reduction Reaction. ChemElectroChem, 2015, 2, 982-987.	1.7	46
395	Effect of Electrolyte pH on the Inherent Electrochemistry of Layered Transitionâ€Metal Dichalcogenides (MoS <sub>2</sub> , MoSe <sub>2</sub> , WS <sub>2</sub> , WSe <sub>2</sub> ). ChemElectroChem, 2015, 2, 1713-1718.	1.7	13
396	Electrochemical Fluorographane: Hybrid Electrocatalysis of Biomarkers, Hydrogen Evolution, and Oxygen Reduction. Chemistry - A European Journal, 2015, 21, 16474-16478.	1.7	14

#	Article	IF	CITATIONS
397	Hydrogenated Graphenes by Birch Reduction: Influence of Electron and Proton Sources on Hydrogenation Efficiency, Magnetism, and Electrochemistry. Chemistry - A European Journal, 2015, 21, 16828-16838.	1.7	26
398	Electrochemistry of Cd <sub>3</sub> As <sub>2</sub> —A 3D Analogue of Graphene. ChemNanoMat, 2015, 1, 359-363.	1.5	2
399	Transitional Metal/Chalcogen Dependant Interactions of Hairpin DNA with Transition Metal Dichalcogenides, MX <sub>2</sub> . ChemPhysChem, 2015, 16, 2304-2306.	1.0	14
400	Definitive Insight into the Graphite Oxide Reduction Mechanism by Deuterium Labeling. ChemPlusChem, 2015, 80, 1399-1407.	1.3	19
401	Frontispiece: Hydrogenated Graphenes by Birch Reduction: Influence of Electron and Proton Sources on Hydrogenation Efficiency, Magnetism, and Electrochemistry. Chemistry - A European Journal, 2015, 21, .	1.7	0
402	Definitive proof of graphene hydrogenation by Clemmensen reduction: use of deuterium labeling. Nanoscale, 2015, 7, 10535-10543.	2.8	15
403	Simultaneous self-exfoliation and autonomous motion of MoS <sub>2</sub> particles in water. Chemical Communications, 2015, 51, 9899-9902.	2.2	13
404	Enhancement of electrochemical and catalytic properties of MoS2 through ball-milling. Electrochemistry Communications, 2015, 54, 36-40.	2.3	51
405	Phase equilibria in the Bi-Sr-Co-O system: Towards the material tailoring of thermoelectric cobaltites. Journal of the European Ceramic Society, 2015, 35, 3005-3012.	2.8	6
406	Cytotoxicity of fluorographene. RSC Advances, 2015, 5, 107158-107165.	1.7	18
407	Enhanced colloidal stability of nanoscale zero valent iron particles in the presence of sodium silicate water glass. Environmental Technology (United Kingdom), 2015, 36, 358-365.	1.2	10
408	Molybdenum Disulfide: Lithium Intercalation Compound Dramatically Influences the Electrochemical Properties of Exfoliated MoS2 (Small 5/2015). Small, 2015, 11, 604-604.	5.2	3
409	GaN:Co epitaxial layers grown by MOVPE. Journal of Crystal Growth, 2015, 414, 62-68.	0.7	1
410	Misfit‣ayered Bi <sub>1.85</sub> Sr <sub>2</sub> Co <sub>1.85</sub> O <sub>7.7â^'<i>δ</i></sub> for the Hydrogen Evolution Reaction: Beyond van der Waals Heterostructures. ChemPhysChem, 2015, 16, 769-774.	1.0	10
411	A limited anodic and cathodic potential window of MoS <sub>2</sub> : limitations in electrochemical applications. Nanoscale, 2015, 7, 3126-3129.	2.8	35
412	Graphene oxide immobilized enzymes show high thermal and solvent stability. Nanoscale, 2015, 7, 5852-5858.	2.8	195
413	Thermodynamic properties of tubular cobaltite Bi3.7Sr11.4Co8O29â^î´Î´. Thermochimica Acta, 2015, 605, 22-27.	1.2	5
414	Synthesis of Strongly Fluorescent Graphene Quantum Dots by Cage-Opening Buckminsterfullerene. ACS Nano, 2015, 9, 2548-2555.	7.3	248

#	Article	IF	CITATIONS
415	Impact Electrochemistry of Layered Transition Metal Dichalcogenides. ACS Nano, 2015, 9, 8474-8483.	7.3	53
416	Tuning of fluorine content in graphene: towards large-scale production of stoichiometric fluorographene. Nanoscale, 2015, 7, 13646-13655.	2.8	153
417	Use of deuterium labelling—evidence of graphene hydrogenation by reduction of graphite oxide using aluminium in sodium hydroxide. RSC Advances, 2015, 5, 18733-18739.	1.7	14
418	Layered titanium diboride: towards exfoliation and electrochemical applications. Nanoscale, 2015, 7, 12527-12534.	2.8	36
419	Insight into the Mechanism of the Thermal Reduction of Graphite Oxide: Deuterium-Labeled Graphite Oxide Is the Key. ACS Nano, 2015, 9, 5478-5485.	7.3	46
420	Sulfur poisoning of emergent and current electrocatalysts: vulnerability of MoS <sub>2</sub> , and direct correlation to Pt hydrogen evolution reaction kinetics. Nanoscale, 2015, 7, 8879-8883.	2.8	17
421	Mo <i><sub>x</sub></i> W <sub>1â^'<i>x</i></sub> S <sub>2</sub> Solid Solutions as 3D Electrodes for Hydrogen Evolution Reaction. Advanced Materials Interfaces, 2015, 2, 1500041.	1.9	49
422	Highly selective removal of Ga 3+ ions from Al 3+ /Ga 3+ mixtures using graphite oxide. Carbon, 2015, 89, 121-129.	5.4	36
423	Preparation of amorphous antimicrobial selenium nanoparticles stabilized by odor suppressing surfactant polysorbate 20. Materials Letters, 2015, 152, 207-209.	1.3	47
424	Catalytic and Charge Transfer Properties of Transition Metal Dichalcogenides Arising from Electrochemical Pretreatment. ACS Nano, 2015, 9, 5164-5179.	7.3	184
425	The dopant type and amount governs the electrochemical performance of graphene platforms for the antioxidant activity quantification. Nanoscale, 2015, 7, 9040-9045.	2.8	19
426	Hydroboration of Graphene Oxide: Towards Stoichiometric Graphol and Hydroxygraphane. Chemistry - A European Journal, 2015, 21, 8130-8136.	1.7	12
427	Fluorographane (C <sub>1</sub> H <sub>x</sub> F <sub>1â^'xâ^'δ</sub> ) <sub>n</sub> : synthesis and properties. Chemical Communications, 2015, 51, 5633-5636.	2.2	34
428	Impact electrochemistry of individual molybdenum nanoparticles. Electrochemistry Communications, 2015, 56, 16-19.	2.3	27
429	Layered transition metal oxyhydroxides as tri-functional electrocatalysts. Journal of Materials Chemistry A, 2015, 3, 11920-11929.	5.2	80
430	Iridium―and Osmiumâ€decorated Reduced Graphenes as Promising Catalysts for Hydrogen Evolution. ChemPhysChem, 2015, 16, 1898-1905.	1.0	29
431	2H → 1T phase transition and hydrogen evolution activity of MoS <sub>2</sub> , MoSe <sub>2</sub> , WS <sub>2</sub> and WSe <sub>2</sub> strongly depends on the MX <sub>2</sub> composition. Chemical Communications, 2015, 51, 8450-8453.	2.2	565
432	High temperature superconducting materials as bi-functional catalysts for hydrogen evolution and oxygen reduction. Journal of Materials Chemistry A, 2015, 3, 8346-8352.	5.2	25

#	Article	IF	CITATIONS
433	Transition metal dichalcogenides (MoS2, MoSe2, WS2 and WSe2) exfoliation technique has strong influence upon their capacitance. Electrochemistry Communications, 2015, 56, 24-28.	2.3	129
434	Geographical and Geological Origin of Natural Graphite Heavily Influence the Electrical and Electrochemical Properties of Chemically Modified Graphenes. Chemistry - A European Journal, 2015, 21, 8435-8440.	1.7	13
435	Ferromagnetic and paramagnetic magnetization of implanted GaN:Ho,Tb,Sm,Tm films. Journal of Applied Physics, 2015, 117, .	1.1	5
436	Toxicity of layered semiconductor chalcogenides: beware of interferences. RSC Advances, 2015, 5, 67485-67492.	1.7	31
437	Separation of thorium ions from wolframite and scandium concentrates using graphene oxide. Physical Chemistry Chemical Physics, 2015, 17, 25272-25277.	1.3	25
438	Mn doped GaN nanoparticles synthesized by rapid thermal treatment in ammonia. Materials Chemistry and Physics, 2015, 164, 108-114.	2.0	5
439	Electrochemical properties of layered SnO and PbO for energy applications. RSC Advances, 2015, 5, 101949-101958.	1.7	11
440	Simple synthesis of Cr2O3 nanoparticles with a tunable particle size. Ceramics International, 2015, 41, 4644-4650.	2.3	20
441	Voltammetry of Layered Black Phosphorus: Electrochemistry of Multilayer Phosphorene. ChemElectroChem, 2015, 2, 324-327.	1.7	97
442	Structure, oxygen non-stoichiometry and thermal properties of (Bi0.4Sr0.6)Sr2CoO5–δ. Thermochimica Acta, 2015, 600, 89-94.	1.2	9
443	Inherent Electrochemistry of Layered Postâ€Transition Metal Halides: The Unexpected Effect of Potential Cycling of PbI <sub>2</sub> . Chemistry - A European Journal, 2015, 21, 3073-3078.	1.7	10
444	Phase diagram of the Sr–Co–O system. Journal of the European Ceramic Society, 2015, 35, 935-940.	2.8	26
445	Exfoliated transition metal dichalcogenides (MoS2, MoSe2, WS2, WSe2): An electrochemical impedance spectroscopic investigation. Electrochemistry Communications, 2015, 50, 39-42.	2.3	62
446	Synthesis of MnO, Mn2O3 and Mn3O4 nanocrystal clusters by thermal decomposition of manganese glycerolate. Ceramics International, 2015, 41, 595-601.	2.3	43
447	Towards graphene iodide: iodination of graphite oxide. Nanoscale, 2015, 7, 261-270.	2.8	54
448	Phase equilibria in the Zn–Mn–O system. Journal of the European Ceramic Society, 2015, 35, 555-560.	2.8	10
449	Lithium Intercalation Compound Dramatically Influences the Electrochemical Properties of Exfoliated MoS <sub>2</sub> . Small, 2015, 11, 605-612.	5.2	250
450	Electrochemistry of Transition Metal Dichalcogenides: Strong Dependence on the Metal-to-Chalcogen Composition and Exfoliation Method. ACS Nano, 2014, 8, 12185-12198.	7.3	288

#	Article	IF	CITATIONS
451	Graphene: Oxygen-Free Highly Conductive Graphene Papers (Adv. Funct. Mater. 31/2014). Advanced Functional Materials, 2014, 24, 4877-4877.	7.8	4
452	Synthesis of InN nanoparticles by rapid thermal ammonolysis. Journal of Nanoparticle Research, 2014, 16, 1.	0.8	2
453	CoO and Co3O4 nanoparticles with a tunable particle size. Ceramics International, 2014, 40, 12591-12595.	2.3	47
454	Concurrent Phosphorus Doping and Reduction of Graphene Oxide. Chemistry - A European Journal, 2014, 20, 4284-4291.	1.7	46
455	Water-soluble highly fluorinated graphite oxide. RSC Advances, 2014, 4, 1378-1387.	1.7	69
456	Transition Metalâ€Depleted Graphenes for Electrochemical Applications via Reduction of CO <sub>2</sub> by Lithium. Small, 2014, 10, 1529-1535.	5.2	30
457	Layered transition metal dichalcogenides for electrochemical energy generation and storage. Journal of Materials Chemistry A, 2014, 2, 8981-8987.	5.2	552
458	Oxygenâ€Free Highly Conductive Graphene Papers. Advanced Functional Materials, 2014, 24, 4878-4885.	7.8	42
459	Cytotoxicity of halogenated graphenes. Nanoscale, 2014, 6, 1173-1180.	2.8	36
460	Highly hydrogenated graphene via active hydrogen reduction of graphene oxide in the aqueous phase at room temperature. Nanoscale, 2014, 6, 2153-2160.	2.8	49
461	Chemical Preparation of Graphene Materials Results in Extensive Unintentional Doping with Heteroatoms and Metals. Chemistry - A European Journal, 2014, 20, 15760-15767.	1.7	39
462	Carbon fragments are ripped off from graphite oxide sheets during their thermal reduction. New Journal of Chemistry, 2014, 38, 5700-5705.	1.4	37
463	Iridium atalystâ€Based Autonomous Bubbleâ€Propelled Graphene Micromotors with Ultralow Catalyst Loading. Chemistry - A European Journal, 2014, 20, 14946-14950.	1.7	25
464	Precise Tuning of the Charge Transfer Kinetics and Catalytic Properties of MoS <sub>2</sub> Materials via Electrochemical Methods. Chemistry - A European Journal, 2014, 20, 17426-17432.	1.7	73
465	Nitrogen doped graphene: influence of precursors and conditions of the synthesis. Journal of Materials Chemistry C, 2014, 2, 2887-2893.	2.7	61
466	Synthesis, magnetic and transport properties of oxygen-free CrN ceramics. Journal of the European Ceramic Society, 2014, 34, 4131-4136.	2.8	19
467	MoS <sub>2</sub> exhibits stronger toxicity with increased exfoliation. Nanoscale, 2014, 6, 14412-14418.	2.8	162
468	Neutron diffraction as a precise and reliable method for obtaining structural properties of bulk quantities of graphene. Nanoscale, 2014, 6, 13082-13089.	2.8	38

#	Article	IF	CITATIONS
469	Towards Graphane Applications in Security: The Electrochemical Detection of Trinitrotoluene in Seawater on Hydrogenated Graphene. Electroanalysis, 2014, 26, 62-68.	1.5	32
470	Alternating Misfit Layered Transition/Alkaline Earth Metal Chalcogenide Ca <sub>3</sub> Co <sub>4</sub> O <sub>9</sub> as a New Class of Chalcogenide Materials for Hydrogen Evolution. Chemistry of Materials, 2014, 26, 4130-4136.	3.2	68
471	Highly selective uptake of Ba <sup>2+</sup> and Sr <sup>2+</sup> ions by graphene oxide from mixtures of IIA elements. RSC Advances, 2014, 4, 26673-26676.	1.7	21
472	Towards graphene bromide: bromination of graphite oxide. Nanoscale, 2014, 6, 6065-6074.	2.8	109
473	Synthetic routes contaminate graphene materials with a whole spectrum of unanticipated metallic elements. Proceedings of the National Academy of Sciences of the United States of America, 2014, 111, 13774-13779.	3.3	133
474	Uranium- and Thorium-Doped Graphene for Efficient Oxygen and Hydrogen Peroxide Reduction. ACS Nano, 2014, 8, 7106-7114.	7.3	73
475	Heat capacity, enthalpy and entropy of Sr14Co11O33 and Sr6Co5O15. Thermochimica Acta, 2014, 575, 167-172.	1.2	16
476	Towards highly electrically conductive and thermally insulating graphene nanocomposites: Al <sub>2</sub> O <sub>3</sub> –graphene. RSC Advances, 2014, 4, 7418-7424.	1.7	50
477	Cytotoxicity Profile of Highly Hydrogenated Graphene. Chemistry - A European Journal, 2014, 20, 6366-6373.	1.7	35
478	Magnetic control of electrochemical processes at electrode surface using iron-rich graphene materials with dual functionality. Nanoscale, 2014, 6, 7391-7396.	2.8	13
479	Cytotoxicity of Exfoliated Transitionâ€Metal Dichalcogenides (MoS <sub>2</sub> , WS <sub>2</sub> , and) Tj ETG 2014, 20, 9627-9632.	Qq1 1 0.78 1.7	34314 rgBT /( 358
480	Capacitance of p―and nâ€Doped Graphenes is Dominated by Structural Defects Regardless of the Dopant Type. ChemSusChem, 2014, 7, 1102-1106.	3.6	45
481	Fluorographenes via thermal exfoliation of graphite oxide in SF <sub>6</sub> , SF <sub>4</sub> and MoF <sub>6</sub> atmospheres. Journal of Materials Chemistry C, 2014, 2, 5198-5207.	2.7	30
482	3D-graphene for electrocatalysis of oxygen reduction reaction: Increasing number of layers increases the catalytic effect. Electrochemistry Communications, 2014, 46, 148-151.	2.3	34
483	Vacuum-assisted microwave reduction/exfoliation of graphite oxide and the influence of precursor graphite oxide. Carbon, 2014, 77, 508-517.	5.4	61
484	Frontispiece: Iridium-Catalyst-Based Autonomous Bubble-Propelled Graphene Micromotors with Ultralow Catalyst Loading. Chemistry - A European Journal, 2014, 20, n/a-n/a.	1.7	0
485	Boron-doped graphene and boron-doped diamond electrodes: detection of biomarkers and resistance to fouling. Analyst, The, 2013, 138, 4885.	1.7	59
486	Transition Metal (Mn, Fe, Co, Ni)â€Đoped Graphene Hybrids for Electrocatalysis. Chemistry - an Asian Journal, 2013, 8, 1295-1300.	1.7	78

#	Article	IF	CITATIONS
487	Potassium assisted reduction and doping of graphene oxides: towards faster electron transfer kinetics. RSC Advances, 2013, 3, 10900.	1.7	7
488	Boron-Doped Graphene: Scalable and Tunable p-Type Carrier Concentration Doping. Journal of Physical Chemistry C, 2013, 117, 23251-23257.	1.5	108
489	Highly Hydrogenated Graphene through Microwave Exfoliation of Graphite Oxide in Hydrogen Plasma: Towards Electrochemical Applications. Chemistry - A European Journal, 2013, 19, 15583-15592.	1.7	48
490	Boron and nitrogen doping of graphene via thermal exfoliation of graphite oxide in a BF3 or NH3 atmosphere: contrasting properties. Journal of Materials Chemistry A, 2013, 1, 13146.	5.2	72
491	Unusual Inherent Electrochemistry of Graphene Oxides Prepared Using Permanganate Oxidants. Chemistry - A European Journal, 2013, 19, 12673-12683.	1.7	86
492	Carcinogenic Organic Residual Compounds Readsorbed on Thermally Reduced Graphene Materials are Released at Low Temperature. Chemistry - A European Journal, 2013, 19, 14446-14450.	1.7	6
493	Rapid thermal synthesis of GaN nanocrystals and nanodisks. Journal of Nanoparticle Research, 2013, 15, 1.	0.8	4
494	Preparation and luminescent properties of cubic potassium-erbium fluoride nanoparticles. Journal of Fluorine Chemistry, 2013, 156, 363-366.	0.9	6
495	Nano-crystals of various lanthanide fluorides prepared using the ionic liquid bmimPF6. Journal of Fluorine Chemistry, 2013, 149, 13-17.	0.9	12
496	Biomarkers Detection on Hydrogenated Graphene Surfaces: Towards Applications of Graphane in Biosensing. Electroanalysis, 2013, 25, 703-705.	1.5	31
497	Large-scale quantification of CVD graphene surface coverage. Nanoscale, 2013, 5, 2379.	2.8	47
498	Purification of carbon nanotubes by high temperature chlorine gas treatment. Physical Chemistry Chemical Physics, 2013, 15, 5615.	1.3	31
499	Searching for Magnetism in Hydrogenated Graphene: Using Highly Hydrogenated Graphene Prepared <i>via</i> Birch Reduction of Graphite Oxides. ACS Nano, 2013, 7, 5930-5939.	7.3	149
500	Complex organic molecules are released during thermal reduction of graphite oxides. Physical Chemistry Chemical Physics, 2013, 15, 9257.	1.3	32
501	Sulfur-Doped Graphene <i>via</i> Thermal Exfoliation of Graphite Oxide in H <sub>2</sub> S, SO <sub>2</sub> , or CS <sub>2</sub> Gas. ACS Nano, 2013, 7, 5262-5272.	7.3	321
502	Halogenation of Graphene with Chlorine, Bromine, or Iodine by Exfoliation in a Halogen Atmosphere. Chemistry - A European Journal, 2013, 19, 2655-2662.	1.7	143
503	High-pressure hydrogenation of graphene: towards graphane. Nanoscale, 2012, 4, 7006.	2.8	78
504	Graphite Oxides: Effects of Permanganate and Chlorate Oxidants on the Oxygen Composition. Chemistry - A European Journal, 2012, 18, 13453-13459.	1.7	156

#	Article	IF	CITATIONS
505	Graphane electrochemistry: Electron transfer at hydrogenated graphenes. Electrochemistry Communications, 2012, 25, 58-61.	2.3	21
506	Inherently Electroactive Graphene Oxide Nanoplatelets As Labels for Single Nucleotide Polymorphism Detection. ACS Nano, 2012, 6, 8546-8551.	7.3	113
507	Influence of parent graphite particle size on the electrochemistry of thermally reduced graphene oxide. Physical Chemistry Chemical Physics, 2012, 14, 12794.	1.3	28
508	Residual strain in recessed AlGaN/GaN heterostructure fieldâ€effect transistors evaluated by micro photoluminescence measurements. Physica Status Solidi C: Current Topics in Solid State Physics, 2012, 9, 911-914.	0.8	6
509	Graphenes prepared by Staudenmaier, Hofmann and Hummers methods with consequent thermal exfoliation exhibit very different electrochemical properties. Nanoscale, 2012, 4, 3515.	2.8	363
510	Chemically reduced graphene contains inherent metallic impurities present in parent natural and synthetic graphite. Proceedings of the National Academy of Sciences of the United States of America, 2012, 109, 12899-12904.	3.3	195
511	Noble metal (Pd, Ru, Rh, Pt, Au, Ag) doped graphene hybrids for electrocatalysis. Nanoscale, 2012, 4, 5002.	2.8	214
512	Graphene Sheet Orientation of Parent Material Exhibits Dramatic Influence on Graphene Properties. Chemistry - an Asian Journal, 2012, 7, 2367-2372.	1.7	23
513	Graphene materials preparation methods have dramatic influence upon their capacitance. Electrochemistry Communications, 2012, 14, 5-8.	2.3	96
514	Metallic Impurities in Graphenes Prepared from Graphite Can Dramatically Influence Their Properties. Angewandte Chemie - International Edition, 2012, 51, 500-503.	7.2	164
515	Chemically-modified graphenes for oxidation of DNA bases: analytical parameters. Analyst, The, 2011, 136, 4738.	1.7	38
516	Electrochemistry at Chemically Modified Graphenes. Chemistry - A European Journal, 2011, 17, 10763-10770.	1.7	288
517	Influence of different SiC surface treatments performed prior to Ni ohmic contacts formation. Microelectronic Engineering, 2011, 88, 553-556.	1.1	4
518	Flux growth of ZnO crystals doped by transition metals. Journal of Crystal Growth, 2011, 314, 123-128.	0.7	10
519	Oxidized Al Film as an Insulation Layer in AlGaN/GaN Metal–Oxide–Semiconductor Heterostructure Field Effect Transistors. Japanese Journal of Applied Physics, 2010, 49, 046504.	0.8	5
520	Femtosecond and highly sensitive GaAs metal–semiconductor–metal photodetectors grown on aluminum mirrors/pseudo-substrates. Semiconductor Science and Technology, 2010, 25, 075001.	1.0	16
521	In-situ doping and implantation of GaN layers with Mn. Physica Status Solidi C: Current Topics in Solid State Physics, 2009, 6, S646-S649.	0.8	5
522	Growth and characterization of GaN:Mn layers by MOVPE. Journal of Crystal Growth, 2008, 310, 5025-5027.	0.7	6

#	Article	IF	CITATIONS
523	Synthesis of Er-complexes for photonic applications. Journal of Physics and Chemistry of Solids, 2007, 68, 1272-1275.	1.9	0
524	Investigation of AlN growth on sapphire substrates in a horizontal MOVPE reactor. Journal of Physics and Chemistry of Solids, 2007, 68, 1131-1134.	1.9	1
525	Porous glass doping by Er3+ for photonics applications. Journal of Materials Science: Materials in Electronics, 2007, 18, 379-382.	1.1	0
526	Growth and properties of GaN and AlN layers on silver substrates. Applied Physics Letters, 2005, 87, 212109.	1.5	16
527	Bipolar Electrochemistry as a Simple Synthetic Route toward Nanoscale Transition of Mo <sub>2</sub> B <sub>5</sub> and W <sub>2</sub> B <sub>5</sub> for Enhanced Hydrogen Evolution Reaction. ACS Sustainable Chemistry and Engineering, 0, , .	3.2	6
528	Graphene and other two-dimensional materials in electrocatalysis. , 0, , .		0
529	Multifunctional Photoelectroactive Platform for CO2 Reduction toward C2+ Products─Programmable Selectivity with a Bioinspired Polymer Coating, ACS Catalysis, 0. , 1558-1571.	5.5	9